iScience

CellPress
OPEN ACCESS

Article

Multi-responsive, flexible, and structurally colored film based on a 1D diffraction grating structure

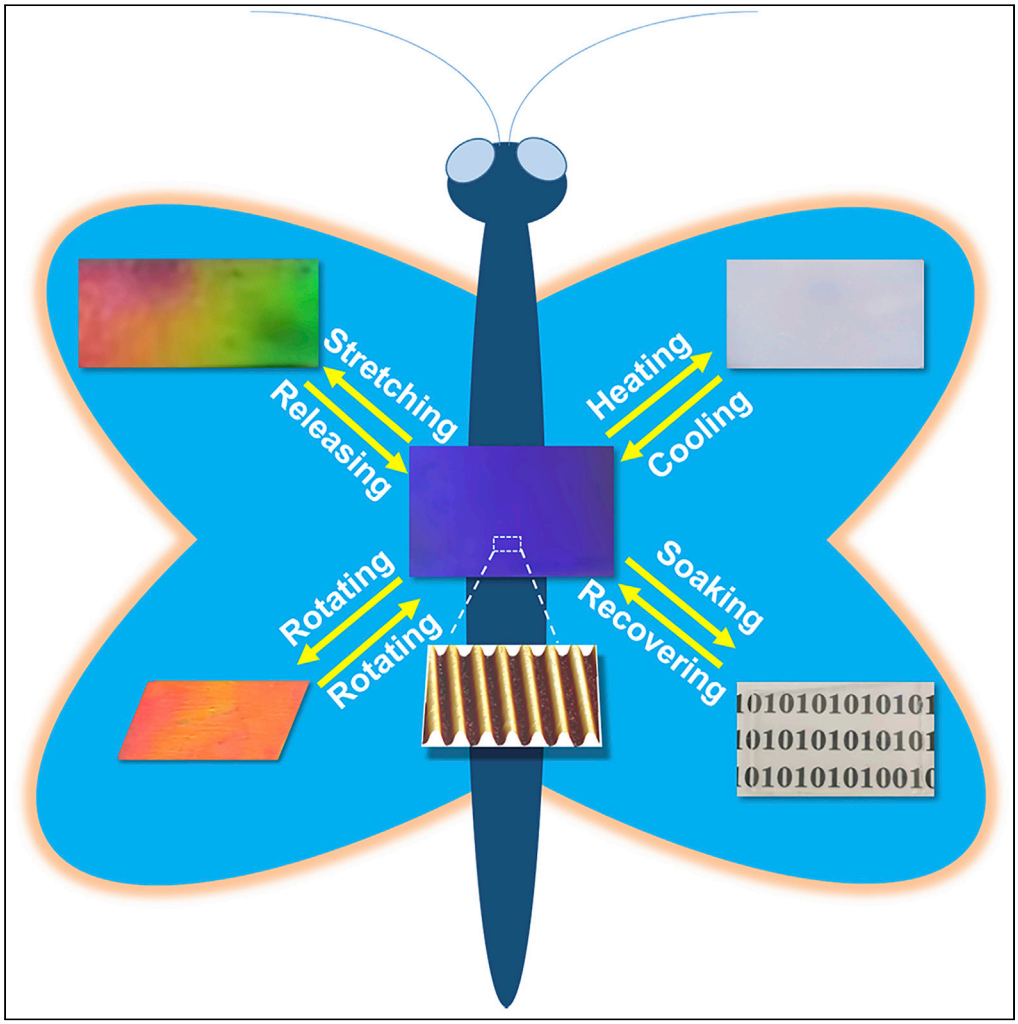

Xiaoxiang Wen, Xuegang Lu, Jianing Li, Chaoping Wei, Hongji Qin, Yuting Liu, Sen Yang

xglu@mail.xjtu.edu.cn (X.L.)
yangsen@mail.xjtu.edu.cn (S.Y.)

Highlights

Multi-responsive hydrogel film with surface 1D grating structure is fabricated

The hydrogel film shows reversible color change during stretching and releasing

The film can be switched between colored and opaque white with temperature

The film can be switched between colored and transparent states using a solvent

Wen et al., iScience 25, 104157
April 15, 2022
https://doi.org/10.1016/j.isci.2022.104157

iScience

CellPress
OPEN ACCESS

Article

Multi-responsive, flexible, and structurally colored film based on a 1D diffraction grating structure

Xiaoxiang Wen,[1] Xuegang Lu,[1,2,*] Jianing Li,[1] Chaoping Wei,[1] Hongji Qin,[1] Yuting Liu,[1] and Sen Yang[1,*]

SUMMARY

In nature, many organisms (e.g., chameleons) protect themselves by changing their colors in response to environmental changes. Inspired by these organisms, we present a multi-responsive, flexible, and structurally colored hydrogel film with a one-dimensional (1D) ordered periodic groove structure. The groove structure endows the film with bright, highly angle-dependent structural colors, which can be reversibly tuned by stretching and releasing. In addition, because of the thermosensitive properties of the hydrogel, the film can be switched between colored state and opaque white state with temperature. In addition, the optical state of the film is sensitive to solvent and can be reversibly changed between colored state and transparent state with soaking and evaporation of the solvent. This reversible, multi-responsive, flexible, and structurally colored hydrogel film has great potential to be used in the fields of color display, sensors, anti-counterfeiting, and so on because of its flexible and diverse tuning methods, excellent optical performance, and convenient preparation process.

INTRODUCTION

Structural color arises from the interaction of complex light with spatially ordered or quasi-amorphous nanostructures or microstructures, including scattering, diffraction, interference, and reflection of light (Eskew, 2002; Takeoka, 2012; Wu et al., 2020a; Kinoshita and Yoshioka, 2005; Chu et al., 2019; Chen et al., 2021). Structural colors are ubiquitous in nature and daily life, such as birds (Stavenga et al., 2011; Michelson, 1911), insects (Hsiung et al., 2017; Biró et al., 2007), reptiles (Teyssier et al., 2015), petals (Whitney et al., 2009), rainbows, and compact discs (Whitney et al., 2009). Inspired by these models, a series of materials have been developed to mimic these structures for applications such as coating (Wen et al., 2021), textile (Wang et al., 2019), display (Ohtsuka et al., 2015; Bechinger et al., 1996; Wang et al., 2015), sensor (Zhang et al., 2018; Kou et al., 2019; Li et al., 2020), and anti-counterfeiting (Heo et al., 2016; Yao et al., 2021). Especially, reversible stimuli-responsive structural colors have received much attention in recent years because of their ability to exhibit a specific color in a particular situation. In the past several years, great efforts have been devoted to fabricating responsive structural color materials. For example, Ahn et al. designed cone-shaped nanostructure arrays on the surface of elastomeric substrates, and the diffraction color can be adjusted according to the change in grating spacing by stretching or compressing the substrate. As-obtained structurally colored elastomeric material that can respond to mechanical stimuli can be used in stretchable and shear strain sensors (Quan et al., 2020). Ge et al. engineered liquid photonic crystal structure arrays using colloidal particles with charged surfaces, and because of the intrinsic relationship between the applied electric field strength and the lattice constants, these liquid PCs exhibit various structural colors in the visible spectrum under different electric fields, which can be used in reflective color displays (Fu et al., 2018). Sun et al. fabricated reversible wrinkled material on a polydimethylsiloxane surface that has a significant variation in transmittance between the wetted and dry states. This solvent-stimulated transmittance variation can be used for smart displays (Wu et al., 2020b). Nevertheless, the structural color of most of the aforementioned materials can only respond to a single stimulus. Realizing multiple responses of optical properties can not only greatly improve the optical performance of materials but also can provide more flexible choices for the design and application of related devices and has become an important development trend. Some efforts have been made to realize the multiple-response of structural colors. Chen et al. reported a triphase microfluidic strategy for the construction of Janus suprabeads with a temperature-magnetic-optical triple response (Wang et al., 2015). Wu et al. developed the temperature-mechanical dual-responsive photonic crystal consisting of a non-compact stack of ZnS nanospheres and polymers (Wu et al., 2021). Jiang et al. have constructed a dynamic double interpenetrating polymer

[1]School of Physics, MOE Key Laboratory for Nonequilibrium Synthesis and Modulation of Condensed Matter, Xi'an Jiaotong University, Xi'an 710049, People's Republic of China

[2]Lead contact

*Correspondence: xglu@mail.xjtu.edu.cn (X.L.), yangsen@mail.xjtu.edu.cn (S.Y.)

https://doi.org/10.1016/j.isci.2022.104157

network as the top layer of a typical bilayer system to create redox, light, and thermal responsive wrinkles (Zhou et al., 2019). Its transparent and opaque optical states can be switched by changing the wrinkle structure through the three stimuli mentioned previously. Switching between multiple optical states under multiple stimuli using a single material is still facing great challenges.

Herein, we present a facile strategy to achieve a multi-responsive, flexible, and structurally colored hydrogel film. Using CD-R discs as a template, its ordered groove structure is replicated on the poly (N-isopropylacrylamide) (PNIPAM)-based hydrogel film. The as-prepared film exhibits bright and highly angle-dependent structural colors. As the viewing angle increases, the film transforms from a transparent state to a colored state. Moreover, the optical performance of the film shows reversible thermo-response, and with the increase in temperature, the film gradually changes from a structurally colored state to a white opaque state. In addition, the hydrogel film possesses good mechanical strength and elasticity, so that reversible modulation of structural color is achieved during stretching and releasing. In addition, the optical state of the film is sensitive to solvent. When the grooves are infiltrated by solvent, the film becomes transparent and the structural color disappears, and then the structural color recovers after the evaporation of the solvent. This 1D grating-structure-based NIPAM film that can switch between transparent, structurally colored state, and white opaque state has not been reported before and has great potential to be used in the fields of color display, sensors, anti-counterfeiting, and so on because of its flexible tuning modes, excellent optical performance, and convenient fabrication process.

RESULTS AND DISCUSSION

The multi-responsive structurally colored film is achieved by replicating the surface groove structure on the hydrogel film membrane using CD-R discs as a template. First, hydrogel precursors were prepared by adding acrylic acid (AA) and $AlCl_3$ into the NIPAM monomer. The purpose of adding AA and $AlCl_3$ is to improve the flexibility and elasticity of the hydrogel film. Then, the NIPAM-AA-Al solution was cast onto the CD-R template. After UV curing, the hydrogel film was carefully peeled off from the template and the hydrogel film with inverse groove structure was obtained. The process is shown in Figure 1A. The inverse groove structure was characterized using AFM technique. Figures 1B and 1C show the top view and 3D AFM image of hydrogel film, which displays the typical uniform 1D periodic groove structure. Numerical analysis in Figure 1D reveals that the periodic width of the 1D-ordered groove array is about 1.5 μm and the maximum depth is about 160 nm, demonstrating a sinusoidal grating structure. It can be further seen from the optical microscopic image in Figure S1 that the film has a 1D-ordered structure with straight grooves parallel to each other over a large area. The as-prepared PNIPAM-AA-Al hydrogel film presents excellent flexibility and elasticity and can withstand repeated stretching and twisting without damage, as shown in Figure 1E. More interestingly, the flexible hydrogel film exhibits bright structural color under ambient light irradiation, and its structural color can be tuned by multiple modes. As shown in Figure 1F, the structural color of the film is not only sensitive to ambient temperature and mechanical tension but also changes with the observation angle and surface wetting state.

It is well-known that structural color arises from complex interactions of light with spatially ordered nanoarrays or microarrays, including diffraction, interference, scattering, and reflection of light (Li et al., 2021a, 2021b). For the aforementioned hydrogel film with a sinusoidal grating structure, the generation of structural color is attributed to the grating diffraction of visible light. As shown in Figure 2, when white light is incident on the grating at a certain angle, the diffracted light on each unit interferes with the other. As the optical path difference of diffracted light of different wavelengths equals an integral time of the wavelength, the coherence is strengthened. The simple law of diffraction can be expressed by the grating equation (Yu et al., 2010)

$$\sin(\theta_m) - \sin(\theta_i) = \frac{m\lambda}{d} \qquad \text{(Equation 1)}$$

where θ_i and θ_m are the angles of incidence and diffraction, respectively, and m is the diffraction order. λ denotes the wavelength of the incident light, and d represents the period of the grating. For the sinusoidal grating structure, the diffraction is strengthened only when the diffraction order m is 0, ± 1, and the diffraction of other orders is offset. For $m = 0$, all wavelengths of light are coherently strengthened at the angle of $\theta_0 = \theta_i$, and what can be observed from this angle is still white. For $m = \pm 1$, the diffraction angle, $\theta_{\pm 1}$, corresponding to the coherence enhancement of light of different wavelengths varies; i.e., in the visible light range, as the wavelength increases, the diffraction angle $\theta_{\pm 1}$ gradually increases, so that white light is decomposed into the light of different wavelengths to produce structural colors.

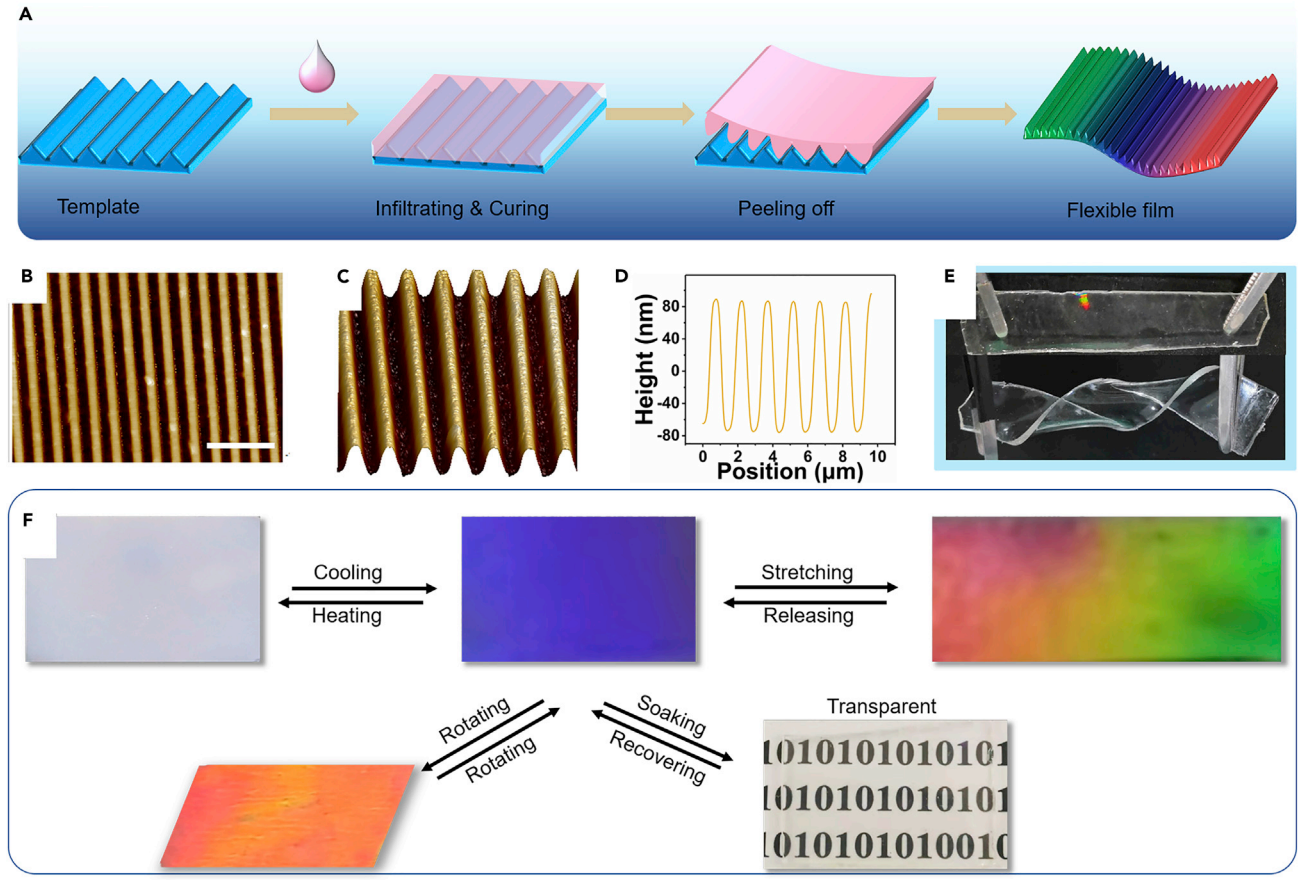

Figure 1. Fabrication of multi-responsive flexible hydrogel film

(A) Scheme of the procedure to prepare the PNIPAM-AA-Al hydrogel film.

(B–D) AFM images of surface groove structure of the hydrogel film, and D) corresponding numerical analysis. The scale bar in B is 5 μm.

(E) Digital photographs revealing the mechanical elasticity and flexibility of PNIPAM-AA-Al hydrogel film.

(F) Multi-responsive behavior of the hydrogel film. (See also Figure S1).

Obviously, it can be predicted that the structural color of as-prepared hydrogel film with sinusoidal grating structure is significantly angular dependent, as shown in Figure 3 and Video S1. It can be seen from Figure 3 that when the viewing angle is 0°, the hydrogel film with the panda pattern is in a transparent state. As the viewing angle increases from 11° to 29°, the panda pattern changes from bright indigo to green and red colors. Figure 3B shows the corresponding reflection spectra with peak wavelengths of 452 nm, 525 nm, and 648 nm. The position of the reflection peak changes by 196 nm when the viewing angle increases from 11° to 29°. The angle dependence of optical properties can be illustrated in Figure 3C. When visible light is incident at θ_i angle, the structural color appears because of first-order diffraction in the angle range of θ to $\theta + \Delta\theta$, and the structural color gradually changes from blue to red with the increase of diffraction angle. As the viewing angle is less than θ (*e.g.* 0° in Figure 3A), the hydrogel film appears transparent because the coherence of the visible light does not take place in this range. The color change in a small angle range can be easily observed with the naked eye, which provides a good opportunity for its use in anti-counterfeiting.

Generally, PNIPAM hydrogels are relatively fragile and cannot withstand large tensile deformations. By adding a small amount of AA and Al^{3+} into the NIPAM monomer to modify the network structure of the hydrogel, its strength and elastic deformation ability can be greatly improved (Xia et al., 2019). Besides, the prepared PNIPAM-AA-Al hydrogel film can undergo reversible elastic deformation under the stretching force, causing significant changes in optical properties. Figures 4A1–4E1 show the structural colors of PNIPAM-AA-Al hydrogel film stretched at different ratios. It can be seen that when the stretching ratio

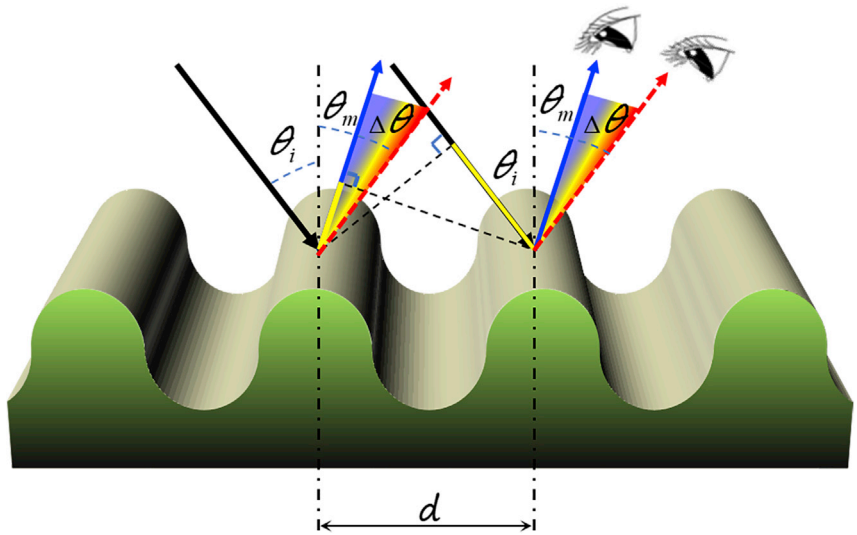

Figure 2. Schematic diagram of coherent diffraction of sinusoidal grating

increases from 0 to 36.5%, the structural color of the hydrogel film gradually changes from the initial pure blue to iridescent color. In the area near the fixed (left) end of the film, the structural color gradually changes from blue (0%) to blue-green (4.5%), green (20.3%), orange (35.3%), and red (36.5%). The process is reversible. With the release of tensile stress, the deformation of the hydrogel film decreases, and the structural color gradually returns to its initial state. This mechanical response of structural color is vividly shown in

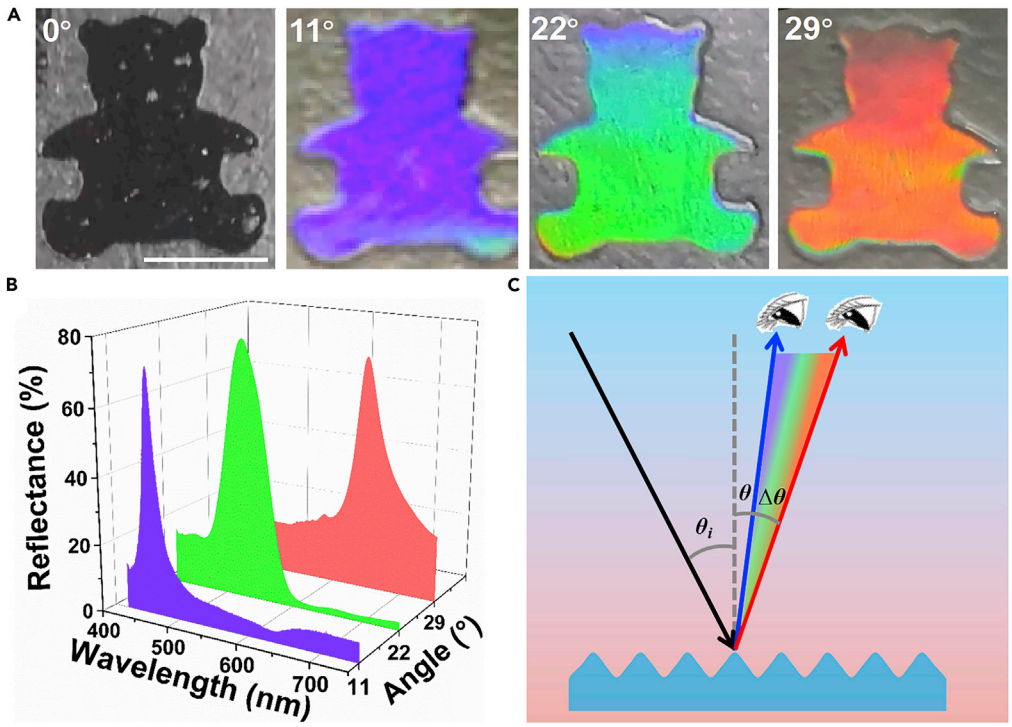

Figure 3. Angular dependence of PNIPAM-AA-Al hydrogel film

(A) Digital photographs of the structural colors in the PNIPAM-AA-Al hydrogel film at various angles.

(B) The reflection spectra corresponding to each angle in (A).

(C) The relationship between the angle dependence of optical characteristics and grating diffraction. The scale bar in (A) is 0.5 cm.

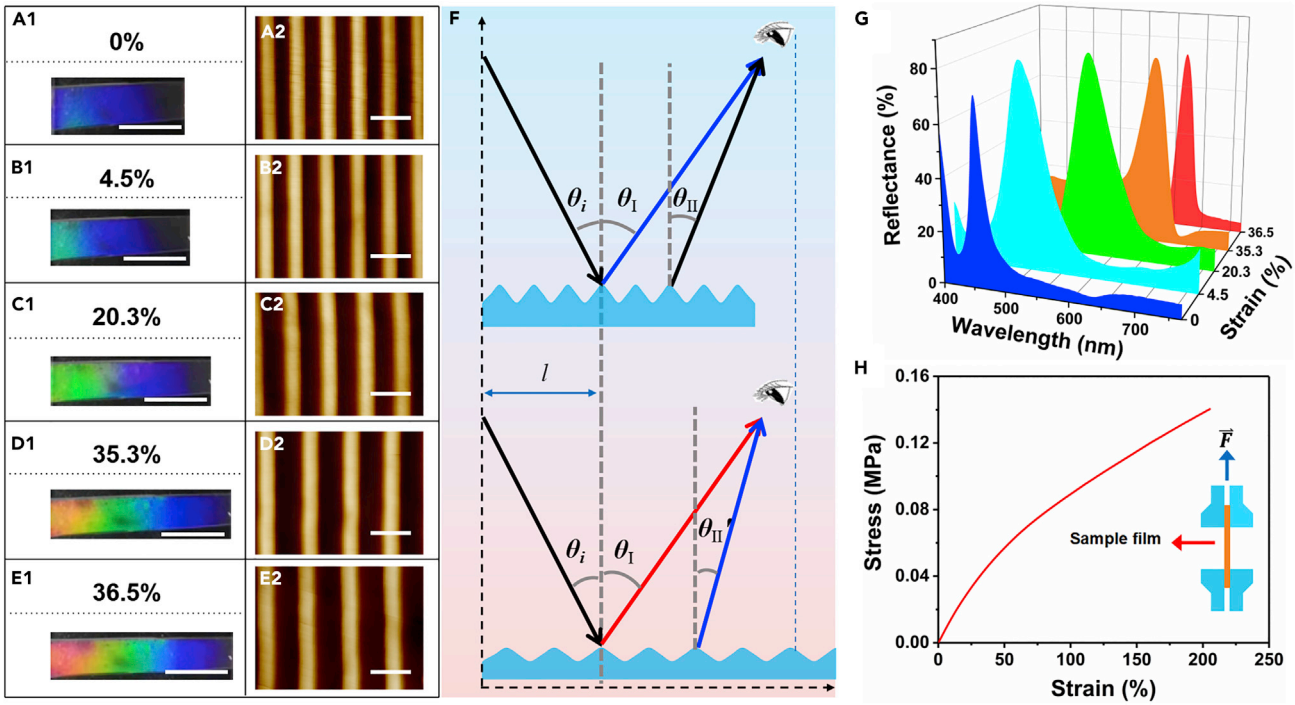

Figure 4. Mechanical response of structural colors of PNIPAM-AA-Al hydrogel film

(A1–E1) Structural colors of the PNIPAM-AA-Al hydrogel film under various stretching ratios (from 0% to 36.5%).

(A2–E2) AFM images of grating structure corresponding to the various stretching ratios. The scale bars of A1-E1 and A2–E2 are 1 cm and 2 μm, respectively.

(F) Schematic illustration of the color change in the hydrogel film during stretching.

(G) Reflection spectra of PNIPAM-AA-Al hydrogel film corresponding to the various stretching ratios.

(H) Stress-strain curve of PNIPAM-AA-Al hydrogel film. (See also Figure S2).

Videos S2. It is conceivable that this process should be related to the changes in the grating structure caused by the stretching process. Figure 4A2–4E2 show the AFM results of the hydrogel film stretched at different ratios. It can be seen that the ordered periodic structure remains after stretching, and the grating period increases as the increase of stretching ratios. The grating periods corresponding to each stretching ratio are 1.50 μm (0%), 1.57 μm (4.5%), 1.80 μm (20.3%), 2.02 μm (35.3%), and 2.06 μm (36.5%), respectively. According to the grating equation in formula (1), as the incident angle and diffraction angle remain constant, the wavelengths of light which are coherently strengthened increase with the increase of grating period *d*, causing redshift of the structural color. In addition, the appearance of iridescent color in Figure 4 is not only because of the increase of grating period but is also related to the change of viewing angle relative to the free (right) end of the film. As can be seen from Figure 4F, when the incident angle of the light and the observation position of the human eye are relatively fixed, the diffraction angle, θ_I, of the diffracted light near the fixed end observed by the human eye during the film stretching process is almost unchanged, so that the wavelength of the diffracted light in this region increases with the increase of the grating period. However, in the region near the free end, although the stretching increases the grating period, the diffraction angle $\theta_{II}^{'}$ of the diffracted light decreases continuously, so the wavelength of the diffracted light observed by the human eye changes little, so that the region maintains the initial color. Figure 4G presents the reflectance spectra of the film near the fixed end during stretching. The reflection peak wavelengths are 460 nm (0%), 485 nm (4.5%), 560 nm (20.3%), 640 nm (35.3%), and 665 nm (36.5%), showing an obvious red-shift. To confirm the mechanical properties of PNIPAM-AA-Al hydrogel, tensile tests were carried out on the film. The stress-strain curve in Figure 4H demonstrates excellent elasticity of the film, and the tensile strain can reach at least 206%. Meanwhile, to verify the mechanical stability of the PNIPAM-AA-Al structured colored film, a stretching (36.5%)-relaxing (0%) test was performed on the film, and the reflectance spectra were measured for each state. According to this procedure, reflection spectra were obtained for 100 cycles, as shown in Figure S2. The reflectance spectra were stable with a variation of wavelength within 15 nm for each cyclic state, which indicates that the film was not significantly damaged during the

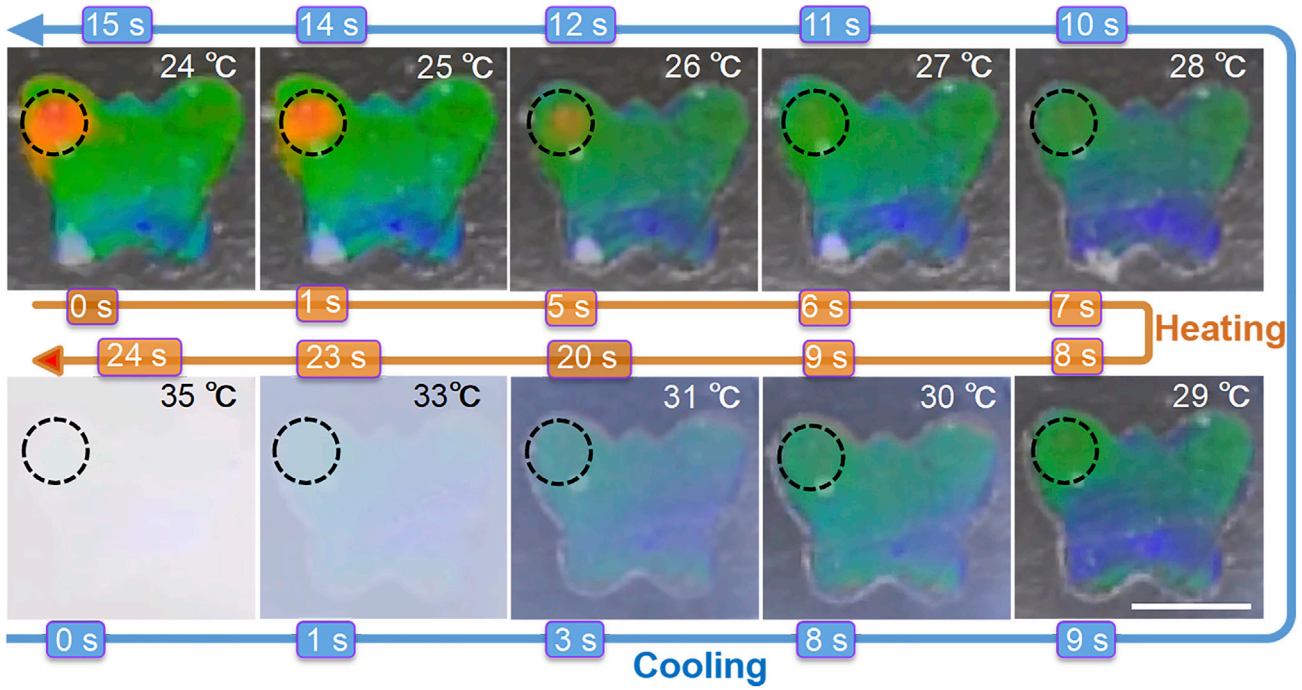

Figure 5. Temperature response of PNIPAM-AA-Al hydrogel film

Digital photographs of the temperature-responsive structural colors in the PNIPAM-AA-Al hydrogel film with increasing the temperature from 24°C to 35°C or vice versa. The scale bar is 0.5 cm. (See also Figures S3 and S4).

stretch-release process; that is, the film has stable mechanical properties. Therefore, the prepared hydrogel film with unique mechanical response optical properties has the potential to be applied for mechanical sensors and so on.

It is well-known that the hydrogel containing the thermosensitive monomer PNIPAM shrinks above the phase transition temperature, resulting in a significant volume change (Xia et al., 2013). This volume change will inevitably lead to the change of the grating structure of the hydrogel membrane and ultimately lead to the change of optical properties. Compared with PNIPAM, the PNIPAM-AA-Al hydrogel still retains thermosensitive properties in addition to its enhanced mechanical properties. To confirm the thermosensitive optical performance of PNIPAM-AA-Al hydrogel film, we prepared a butterfly pattern with grating structure locally on the hydrogel film and recorded the changes of structural color with temperature, as shown in Figure 5. The PNIPAM-AA-Al hydrogel film was placed on a heating plate and a significant temperature response was observed when the temperature of the heating plate was set at 35°C. As can be seen that as the temperature rises from room temperature (24°C) to 35°C, the overall structural color of the butterfly pattern blue-shifts, and the local structural color gradually changes from the initial orange to green (the corresponding reflection peak wavelength decreases from 630 nm to 520 nm (Figure S3), and finally turns white, accompanied by the disappearance of the pattern. In this process, as the temperature increases, the volume of the hydrogel shrinks, resulting in a reduction in the grating period and a blue-shift in the structural color. When the temperature reaches the critical phase transition temperature, a hydrophilic-hydrophobic transition occurs, and the discrete aqueous phases formed in the hydrogel network strongly scatter light, resulting in the concealment of the structural color. The optical photograph of the hydrogel film recorded at 35°C is shown in Figure S4. It is worth noting that the PNIPAM-AA-Al hydrogel film can revert from unpatterned white to a partially green to orange structurally colored butterfly pattern, as the temperature of the heating plate decreases. This is because of the expansion of the PNIPAM-AA-Al hydrogel film with decrease in temperature, resulting in an increase in the grating period. The change in the film because of heating and cooling is reversible and can be repeated many times, as shown in Video S3. Thus, it can be seen that the thermosensitive properties of the synthesized PNIPAM-AA-Al hydrogel film can not only achieve the switching of the light

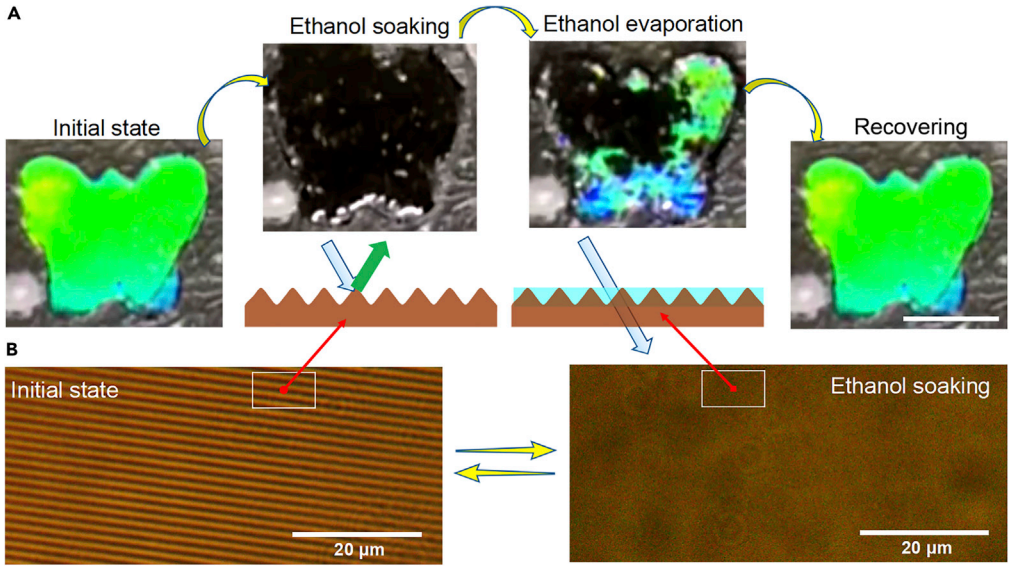

Figure 6. Solvent response of PNIPAM-AA-Al hydrogel film

(A) Digital photographs of PNIPAM-AA-Al hydrogel film in the initial state and after soaking with ethanol and recovering again. The scale bar in A) is 0.5 cm.

(B) Top-view optical microscope images of PNIPAM-AA-Al film in the initial state and under ethanol soaked. The schematic diagram shows the light propagation modes in two states.

transmission but also realize the temperature response of the structural colors, which provides potential to be used as thermal sensors and smart windows with structural colors.

Another interesting phenomenon is that the prepared hydrogel film can respond to solvents and exhibit different optical behaviors. Figure 6A shows the changes in the structural color of hydrogel film before and after soaking with ethanol. Before soaking in ethanol, the butterfly pattern made of the hydrogel film with grating structure showed a bright green color. After soaking with ethanol, the structural color of the butterfly pattern disappears immediately, and the film becomes transparent. Then, with the evaporation of ethanol, the structural color of the pattern gradually appeared and finally returned to the initial state with the complete evaporation of ethanol. This reversible process is vividly demonstrated in Videos S4. Figure 6B shows the top view optical microscopy images of PNIPAM-AA-Al flexible film before and after ethanol soaking. It can be seen that there exists a typical 1D-ordered groove structure on the initial hydrogel film, but this groove structure completely disappears after being soaked with ethanol. That is to say, after filling the grooves with ethanol, the original grating structure disappears because of the similar refractive index between ethanol (1.36) and the PNIPAM-AA-Al hydrogel (1.48, measured at 24°C by Abbe refractometer), which causes the film to become transparent and the structural color disappears. As the ethanol evaporates, the grating structure on the film gradually reappears, so that the structural color also recovers. In addition to ethanol, other solvents which are compatible with PNIPAM (such as water, ethylene glycol, etc.) can make the film demonstrate similar response behaviors. This solvent response characteristic makes the hydrogel film promising for applications in anti-counterfeiting, sensing, and other fields.

CONCLUSION

In conclusion, we present a facile strategy to achieve a multi-responsive structurally colored hydrogel film. This optical film is obtained by replicating the 1D grating structure of the CD-R template to the surface of the PNIPAM-AA-Al hydrogel film. The as-prepared hydrogel film exhibits bright and highly angle-dependent structural colors. The film transforms from a transparent state to a colored state as the viewing angle increases. Moreover, the hydrogel film possesses good mechanical strength and elasticity and demonstrates reversible color change during stretching and releasing. The thermosensitive nature of PNIPAM-AA-Al hydrogel endows the film reversible temperature-responsive optical properties, and with the increase of temperature, the film gradually changes from structural color state to white opaque state.

Furthermore, the optical state of the film is sensitive to solvent. After soaking with a solvent like ethanol, the film becomes transparent and the structural color disappears, and then the structural color recovers after the evaporation of the solvent. This multi-responsive hydrogel film is potentially to be applied in the fields of color display, sensors, anti-counterfeiting, and so on owing to its diverse tuning modes, unique optical performance, and inexpensive manufacturing process.

Limitation of the study

Although in this study the strength and elastic deformability of the hydrogel film were greatly improved by adding small amounts of AA and Al^{3+} to the NIPAM monomer to change the network structure of the hydrogel, which resulted in stronger mechanical properties of the PNIPAM-AA-Al hydrogel film while maintaining thermal sensitivity, the variation ranges of the structural colors induced by thermo-stimuli are still limited. As the temperature increases from room temperature (24°C) to the phase transition temperature (35°C), the structural color of the films changes from the initial orange to green, and the corresponding peak reflection wavelength decreases from 630 nm to 520 nm, and the wavelength variation range is temporarily unable to cover the entire wavelength range of visible light. In addition, as a hydrogel, the stability of PNIPAM-AA-Al is still insufficient, and it is easy to lose water in the air, which may cause adverse effects on subsequent practical applications. Therefore, it is necessary to further improve the stability of the hydrogel in the future.

STAR★METHODS

Detailed methods are provided in the online version of this paper and include the following:

- KEY RESOURCES TABLE
- RESOURCE AVAILABILITY
  - Lead contact
  - Materials availability
  - Data and code availability
- METHOD DETAILS
  - Sample preparation
  - Evaluations

SUPPLEMENTAL INFORMATION

Supplemental information can be found online at https://doi.org/10.1016/j.isci.2022.104157.

ACKNOWLEDGMENTS

This work is supported by the National Natural Science Foundation of China (No. 61975162), the Shaanxi Natural Science Foundation (No. 2020JM-062), the Fundamental Research Funds for the Central Universities (No. xzy022021042), the World-Class Universities (Disciplines), and the Characteristic Development Guidance Funds for the Central Universities. We also acknowledge the testing and analysis support from the Instrument Analysis Center of Xi'an Jiaotong University (China).

AUTHOR CONTRIBUTIONS

X.W. and X.L. conceived the idea. X.W. carried out the main experiment under the supervision of X.L. and S.Y. J. L. and H.Q. helped with the AFM measurements. C.W. and Y. L. helped with the spectroscopy measurements. X.W. wrote the original draft, and X.L. revised the manuscript.

DECLARATION OF INTERESTS

The authors declare no competing interests.

Received: January 10, 2022
Revised: February 28, 2022
Accepted: March 22, 2022
Published: April 15, 2022

REFERENCES

Bechinger, C., Ferrer, S., Zaban, A., Sprague, J., and Gregg, B.A. (1996). Photoelectrochromic windows and displays. Nature *383*, 608–610.

Biró, L.P., Kertész, K., Vértesy, Z., Márk, G.I., Bálint, Z., Lousse, V., and Vigneron, J.P. (2007). Living photonic crystals: butterfly scales — nanostructure and optical properties. Mater. Sci. Eng. C. *27*, 941–946.

Chen, C., Airoldi, C.A., Lugo, C.A., Bay, R.K., Glover, B.J., and Crosby, A.J. (2021). Flower inspiration: broad-angle structural color through tunable hierarchical wrinkles in thin film multilayers. Adv. Funct. Mater. *31*, 2006256.

Chu, G., Camposeo, A., Vilensky, R., Vasilyev, G., Martin, P., Pisignano, D., and Zussman, E. (2019). Printing flowers? Custom-tailored photonic cellulose films with engineered surface topography. Matter *1*, 988–1000.

Eskew, R.T. (2002). The physics and chemistry of color. The fifteen causes of color, second edition. Color Res. Appl. *27*, 377–378.

Fu, Q., Zhu, H., and Ge, J. (2018). Electrically tunable liquid photonic crystals with large dielectric contrast and highly saturated structural colors. Adv. Funct. Mater. *28*, 1804628.

Heo, Y., Kang, H., Lee, J.-S., Oh, Y.-K., and Kim, S.-H. (2016). Lithographically encrypted inverse opals for anti-counterfeiting applications. Small *12*, 3819–3826.

Hsiung, B.-K., Siddique, R.H., Stavenga, D.G., Otto, J.C., Allen, M.C., Liu, Y., Lu, Y.-F., Deheyn, D.D., Shawkey, M.D., and Blackledge, T.A. (2017). Rainbow peacock spiders inspire miniature super-iridescent optics. Nat. Commun. *8*, 2278.

Kinoshita, S., and Yoshioka, S. (2005). Structural colors in nature: the role of regularity and irregularity in the structure. ChemPhysChem *6*, 1442–1459.

Kou, D., Zhang, Y., Zhang, S., Wu, S., and Ma, W. (2019). High-sensitive and stable photonic crystal sensors for visual detection and discrimination of volatile aromatic hydrocarbon vapors. Chem. Eng. J. *375*, 121987.

Li, Z., Liu, Y., Marin, M., and Yin, Y. (2020). Thickness-dependent wrinkling of PDMS films for programmable mechanochromic responses. Nano Res. *13*, 1882–1888.

Li, K., Li, T., Zhang, T., Li, H., Li, A., Li, Z., Lai, X., Hou, X., Wang, Y., Shi, L., et al. (2021a). Facile full-color printing with a single transparent ink. Sci. Adv. *7*, eabh1992.

Li, K., Li, C., Li, H., Li, M., and Song, Y.J.i. (2021b). Designable structural coloration by colloidal particle assembly: from nature to artificial manufacturing. iScience *24*, 102121.

Michelson, A.A. (1911). LXI. On metallic colouring in birds and insects. Lond. Edinb. Dublin Philosophical Mag. J. Sci. *21*, 554–567.

Ohtsuka, Y., Seki, T., and Takeoka, Y. (2015). Thermally tunable hydrogels displaying angle-independent structural colors. Angew. Chem. Int. Ed. *54*, 15368–15373.

Quan, Y.-J., Kim, Y.-G., Kim, M.-S., Min, S.-H., and Ahn, S.-H. (2020). Stretchable biaxial and shear strain sensors using diffractive structural colors. ACS Nano *14*, 5392–5399.

Stavenga, D.G., Leertouwer, H.L., Marshall, N.J., and Osorio, D. (2011). Dramatic colour changes in a bird of paradise caused by uniquely structured breast feather barbules. Proc. Biol. Sci. *278*, 2098–2104.

Takeoka, Y. (2012). Angle-independent structural coloured amorphous arrays. J. Mater. Chem. *22*, 23299–23309.

Teyssier, J., Saenko, S.V., van der Marel, D., and Milinkovitch, M.C. (2015). Photonic crystals cause active colour change in chameleons. Nat. Commun. *6*, 6368.

Whitney, H.M., Kolle, M., Andrew, P., Chittka, L., Steiner, U., and Glover, B.J. (2009). Floral iridescence, produced by diffractive optics, acts as a cue for animal pollinators. Science *323*, 130–133.

Wen, X., Lu, X., Wei, C., Li, J., Li, Y., and Yang, S. (2021). Bright, angle-independent, solvent-responsive, and structurally colored coatings and rewritable photonic paper based on high-refractive-index colloidal quasi-amorphous arrays. ACS Appl. Nano Mater. *4*, 9855–9865.

Wang, X., Li, Y., Zhou, L., Chai, L., Fan, Q., and Shao, J. (2019). Structural colouration of textiles with high colour contrast based on melanin-like nanospheres. Dyes Pigm. *169*, 36–44.

Wang, H., Yang, S., Yin, S.-N., Chen, L., and Chen, S. (2015). Janus suprabead displays derived from the modified photonic crystals toward temperature magnetism and optics multiple responses. ACS Appl. Mater. Inter. *7*, 8827–8833.

Wu, P., Wang, J., and Jiang, L. (2020a). Bio-inspired photonic crystal patterns. Mater. Horiz. *7*, 338–365.

Wu, K., Sun, Y., Yuan, H., Zhang, J., Liu, G., and Sun, J. (2020b). Harnessing dynamic wrinkling surfaces for smart displays. Nano Lett. *20*, 4129–4135.

Wu, Y., Wang, Y., Zhang, S., and Wu, S. (2021). Artificial chameleon skin with super-sensitive thermal and mechanochromic response. ACS Nano *15*, 15720–15729.

Xia, L.-W., Xie, R., Ju, X.-J., Wang, W., Chen, Q., and Chu, L.-Y. (2013). Nano-structured smart hydrogels with rapid response and high elasticity. Nat. Commun. *4*, 2226.

Xia, Y., Chen, B., Gao, S., Liu, Y., Zeng, Z., Cao, M., and Wang, S. (2019). Tough, freestanding, and colorless photonic paper using water as ink. Adv. Mater. Inter. *6*, 1901363.

Yu, C., O'Brien, K., Zhang, Y.-H., Yu, H., and Jiang, H. (2010). Tunable optical gratings based on buckled nanoscale thin films on transparent elastomeric substrates. Appl. Phys. Lett. *96*, 041111.

Yao, W., Lan, R., Li, K., and Zhang, L. (2021). Multiple anti-counterfeiting composite film based on cholesteric liquid crystal and QD materials. ACS Appl. Mater. Inter. *13*, 1424–1430.

Zhang, R., Wang, Q., and Zheng, X. (2018). Flexible mechanochromic photonic crystals: routes to visualised sensors and their mechanical properties. J. Mater. Chem. C *6*, 3182.

Zhou, L., Ma, T., Li, T., Ma, X., Yin, J., and Jiang, X. (2019). Dynamic interpenetrating polymer network (IPN) strategy for multiresponsive hierarchical pattern of reversible wrinkle. ACS Appl. Mater. Inter. *11*, 15977–15985.

STAR★METHODS

KEY RESOURCES TABLE

REAGENT or RESOURCE	SOURCE	IDENTIFIER
Chemicals, peptides, and recombinant proteins		
N-isopropylacrylamide (NIPAM)	Shanghai Aladdin Biochemical Technology Co., Ltd.	CAS: 2210-25-5
Acrylic acid (AA)	Shanghai Aladdin Biochemical Technology Co., Ltd.	CAS: 79-10-7
Ethanol	Shanghai Aladdin Biochemical Technology Co., Ltd.	CAS: 64-17-5
Ethylene glycol	Shanghai Aladdin Biochemical Technology Co., Ltd.	CAS: 107-21-1
Aluminum chloride hexahydrate ($AlCl_3 \cdot 6H_2O$)	Zancheng (Tianjin) Technology Co., Ltd.	CAS: 7784-13-6
2-hydroxy-2-methylpropiophenone (HMPP)	Shanghai Aladdin Biochemical Technology Co., Ltd.	CAS: 7473-98-5
N,N′-Methylenebisacrylamide (BIS)	Shanghai Titan Technology Co., Ltd.	CAS: 110-26-9

RESOURCE AVAILABILITY

Lead contact

Further information and requests for resources and reagents should be directed to and will be fulfilled by the Lead Contact, Xuegang Lu (xglu@mail.xjtu.edu.cn).

Materials availability

This study did not generate new unique reagents.

Data and code availability

- This paper analyzes existing, publicly available data. These accession numbers for the datasets are listed in the key resources table.
- This paper does not report original code.
- Any additional information required to reanalyze the data reported in this paper is available from the lead contact upon request.

METHOD DETAILS

Sample preparation

Template preparation by processing CD-R disc

First, a CD-R disc was cut to a suitable size, and strong tape was stuck on one side of the disc. Then, the tape was torn off to expose the groove structure of the disc. Next, as-obtained disc was ultrasonically treated in ethanol for 30 min, washed with water and ethanol alternately, and dried with a blower. In this way, a template with grooves structure on the surface was obtained.

Fabrication of composite hydrogel film with 1D periodic groove structure

Typically, NIPAM (3.0 g), BIS (60 mg), HMPP (40 μL) were added into the mixed solution composed of ethylene glycol (1.5 mL) and ethanol (1.5 mL) by ultrasonication for 20 min. Then, $AlCl_3 \cdot 6H_2O$ (70 mg) and acryl acid (100 μL) were added into the mixed solution and treated with ultrasonication for 20 min to form a homogeneous solution. The solution was then cast onto the CD-R template and left overnight. The thickness of the liquid film was controlled at 1 mm. Next, the solution was cured after 2 min of UV light exposure. Finally, the cured film was carefully peeled off from the template and soaked in water for 1 h.

Evaluations

The morphologies of the as-prepared products were characterized by atomic force microscopy (AFM, MultiMode 8, Bruker, China). The refractive indexes of ethanol and the PNIPAM-AA-Al hydrogel

were measured at 24°C by Abbe refractometer. The optical reflection spectra of the colored films were recorded using a fiber optic spectrometer (PG2000-Pro, China) in the range of 300–1,000 nm with a resolution of 0.3 nm. The mechanical measurement was performed in a DMA Q800 from TA Instruments.

QUANTIFICATION AND STATISTICAL ANALYSIS

All data were presented as mean values.